

DETERMINATION OF THE IMPURITIES CONCENTRATION IN TUNGSTEN, MOLYBDENUM, TIN, AND TELLURIUM TARGETS USING NEUTRON ACTIVATION ANALYSIS TECHNIQUES

A. El Abd¹, M. Mostafa²

¹Reactor Physics Department, Nuclear Research Centre, Inchass, Egypt

²Radioactiveisotopes and Generators, Hot labs Centre, Inchass, Egypt

The fast and k_0 -neutron activation analysis (k_0 -NAA) methods were used to investigate the radioimpurities concentration of ^{124}Sb , ^{134}Cs , ^{60}Co , ^{87}Rb , ^{182}Ta , ^{233}Pa , ^{65}Zn , ^{56}Fe , $^{110\text{m}}\text{Ag}$, ^{51}Cr , ^{95}Zr , ^{75}Se and $^{114\text{m}}\text{In}$ in the target samples WO_3 , MoO_3 , SnO_2 and TeO_2 which are needed for radioisotopes ^{188}Re , $^{99\text{m}}\text{Tc}$, ($^{113\text{m}}\text{In}$ and $^{117\text{m}}\text{Sn}$) and ^{131}I production respectively at the Second Egyptian Research Reactor (ETR-2). Experimental data, procedures and theoretical treatments were described. The concentrations of radioimpurities were determined and their sources either neutron capture reactions, or threshold reactions or both were identified. The accuracy of the determined concentrations was checked using the IAEA Soil-7 reference sample.

Keywords: impurities, concentration, isotope, fast neutron flux, specific activity, threshold reactions, k_0 -neutron activation analysis, neutron spectrum parameters.

Introduction

Radioisotopes continue to play an important role in the biomedical sciences. Reactor produced radionuclides are widely used in nuclear medicine and represent powerful tools in diagnostic and therapeutic procedures [1, 2]. Impurities are usually found in commercial targets which are used to produce any required isotopes by neutron irradiation. These impurities are formed either by neutron capture reactions or threshold reactions or both reactions. Reduction or elimination of these radioimpurities is essential from the viewpoint of patient safety, since they may co-elute with any specific isotope. So, qualitative and quantitative analysis of these impurities in the neutron-irradiated targets is considered to be an important step before carrying out any purification process prior to preparation of any generator or isotope.

Impurities are most significantly affected by the method of manufacturing the generator or isotope. Näsam and Vayrynen [3] qualitatively studied the impurities in $^{99\text{m}}\text{Tc}$ generators by determining their half lives. Differences were found between generators produced by the same manufactures using the same method. ^{95}Zr , ^{95}Nb , ^{124}Sb , ^{60}Co , etc. are found in some $^{99\text{m}}\text{Tc}$ generators. The radioimpurities: ^{122}Sb , ^{124}Sb , ^{60}Co , ^{65}Zn , ^{59}Fe and ^{54}Mn are found in tin targets for the production of $^{117\text{m}}\text{Sn}$ [4]. Contaminations of the ^{188}Re elute with ^{192}Ir , ^{137}Cs , ^{144}Ce , and ^{103}Ru , ^{106}Ru were reported [5]. The radioimpurities of ^{51}Cr , ^{54}Mn , ^{59}Fe , ^{60}Co , ^{75}Se , $^{110\text{m}}\text{Ag}$, ^{124}Sb and ^{65}Zn were found in the neutron irradiated TeO_2 target [6]. Simple procedures for separation of these radioimpurities from tellurium were reported and such procedures can be used for the purification of the tellurium target from them

before neutron irradiation. Prasad et al. [7] used ICP to determine impurities levels in tellurium target. As, Se, Sb; In and Mn; and fifteen non-volatile elements: Ag, Au, Cd, Co, Cr, Cu, Fe, Ga, In, La, Na, Ni, Sc, W and Zn; were determined in tin by neutron activation analysis [8 - 10]. ^{191}Os and ^{192}Ir radioimpurities were found in W target after neutron irradiation to produce ^{188}Re [11]. Fe, Sn and Cr traces were found in analysis of tungsten using neutron activation analysis [12]. Most of these studies are qualitative; however, the quantitative data are rare and missing in literature. In addition some papers report the results in specific activities only.

This work aims mainly at (i) determination of the concentration of radioimpurities in WO_3 , MoO_3 , TeO_2 and SnO_2 targets using the k_0 -NAA and fast neutron activation analysis (FNAA) methods, (ii) determination of the specific activities of the ^{187}W , ^{188}Re , $^{99\text{m}}\text{Tc}$, $^{113\text{m}}\text{In}$, $^{117\text{m}}\text{Sn}$ and ^{131}I radioisotopes, and the contribution of epithermal neutrons on these specific activities, and (iii) determination the contribution of fast neutrons on specific activities $^{117\text{m}}\text{Sn}$ isotope.

Rhenium-188 (^{188}Re , $t_{1/2} = 16.8$ h) is available from the $^{188}\text{W}/^{188}\text{Re}$ generator system made via double neutron capture on ^{186}W . It is produced from the beta decay of ^{188}W ($t_{1/2} = 69.4$ days). It decays by emission of a high-energy beta at 2.12 MeV and a low-abundance and imageable gamma-ray at 155 keV (15 %) [1, 13, 14]. This radioisotope is considered as a therapeutic agent for the bone pain palliation, synovectomy, and other tumor therapy. A simultaneous imaging is possible since it emits both gamma and beta rays [14].

^{99}Mo ($t_{1/2} = 65.94$ h) is produced by the $^{98}\text{Mo}(n, \gamma)^{99}\text{Mo}$ reaction. It decays by beta emission

(84.7 %) to ^{99m}Tc ($t_{1/2} = 6.015$ h) emitting gamma ray line at 140.5 keV (89 %) [15]. ^{99m}Tc is the most important nuclide used for diagnostic purposes, since radiopharmaceuticals labeled with ^{99m}Tc are employed for > 80 % of nuclear medicine applications, e.g., for detection of lung cancer, cardiac blood pool imaging, liver and spleen scintigraphy, etc. [16].

^{113}Sn is produced by the $^{112}\text{Sn}(n, \gamma)^{113}\text{Sn}$ reaction. It decays with a half-life of 115.1 days to produce the daughter nuclide ^{113m}In . ^{113m}In is a low energy gamma-ray emitter with a half-life of 1.658 h [17]. ^{113m}In has many important medical and industrial applications. For example, ^{113m}In -labeled compounds can be used for lung and liver scanning [18], and for brain imaging applications [19]. It can also be used as a radiotracer to study the flow behavior of crude oil in a battery of industrial crude oil/gas separators in oil industry [20].

^{117m}Sn is characterized with high yield of the conversion electrons, with the energies of 0.126 MeV (64 %) and 0.152 MeV (26.1 %), and the low-energy (158.5 keV) gammas. It can be produced in a nuclear reactor via neutron capture $^{116}\text{Sn}(n, \gamma)$ or via the inelastic neutron scattering $^{117}\text{Sn}(n, n')$ [21, 22, 4]. It is a promising radionuclide for therapeutic applications, since the emitted low energy conversion electrons deposit their energy within a short range (0.22 - 0.29 mm) – shorter than beta rays - and which can destroy tumors with lesser damage to the surrounding tissues. Moreover, the emitted gamma rays allow imaging for targeting and dosimetric purpose [21]. ^{131}I ($t_{1/2} = 8.04$ d) is produced by the neutron irradiation of tellurium according to the scheme [23] shown in Fig 1. ^{131}I is used to diagnose and treat cancers of the thyroid gland. Moreover, thyroid disorders can be imaged [24 - 26].

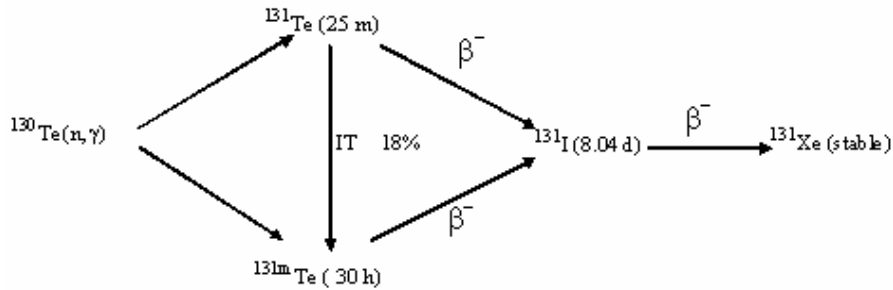


Fig. 1. Production and decay scheme of ^{131}I .

Theoretical treatment

Neutron activation using the k_0 -NAA is widely accepted for multi-element NAA with research reactors [27]. The concentration ρ_a of an analyte ‘‘a’’ in the Høgdahl formalism for which it is required that the cross-section in the thermal neutron energy region varies as $1/v$ (v – neutron velocity), is obtained [27] from its measured activated radioisotope/ gamma ray spectrum as:

$$\rho_a = \left[\frac{N_p/t_m \text{WSDC}}{N_p/t_m \text{WSDC}} \right]_{\text{Au}} \times (1/k_{0 \text{ au}}) \left[\frac{(f + Q_{0, \text{ au}}(\alpha))}{(f + Q_{0, \text{ a}}(\alpha))} \right] \cdot (\mathcal{E}_{p, \text{ au}}/\mathcal{E}_{p, \text{ a}}), \tag{1}$$

where Au refers to the co-irradiated gold monitor and N_p is the net number of counts in the full-energy peak; W - the weight of the sample; w - the weight of the gold monitor; t_m - the measuring time; $S = 1 - \exp(-\lambda t_{\text{irr}})$; λ - the decay constant; t_{irr} - the irradiation time, $D = \exp(-\lambda t_D)$; t_D - the decay time; $C = 1 - \exp(-\lambda t_m)/\lambda t_m$; f - the thermal, ϕ_{th} to epithermal, ϕ_{ep} neutron flux ratio, $Q_0(\alpha) = (I_0(\alpha)/\sigma_0)$ (resonance integral to 2200 ms^{-1} cross-section σ_0) ratio; α - the measure for the epithermal neutron flux distribution, approximated by $1/E^{1 \pm \alpha}$ dependence

[27] with α considered to be independent of neutron energy, \mathcal{E}_p is the full-energy peak detection efficiency and $k_{0 \text{ au}}$ are composite nuclear data constant factors [27, 28]. α and f are the input parameters in the k_0 -NAA and are determined experimentally as follow: the flux ratio f as a function of α is given by the so-called bare bi-isotopic monitor method as

$$f(\alpha) = \left[Q_i(\alpha) - Q_{\text{ref}} \left(\frac{A_{\text{sp}, i}/k_{0, \text{ au}}(i) \mathcal{E}_{p, i}}{A_{\text{sp}, i}/k_{0, \text{ au}}(\text{ref}) \mathcal{E}_{p, \text{ ref}}} \right) \right] \div \left[\left(\frac{A_{\text{sp}, i}/k_{0, \text{ au}}(i) \mathcal{E}_{p, i}}{A_{\text{sp}, i}/k_{0, \text{ au}}(\text{ref}) \mathcal{E}_{p, \text{ ref}}} \right) - 1 \right], \tag{2}$$

where $A_{\text{sp}} = (N_p/t_m \text{WSDC})$, ref refers to a reference isotope, say ^{198}Au , and i refer any other isotopes, $^{95}\text{Zr}/^{95}\text{Nb}$ or $^{97}\text{Zr}/^{97m}\text{Nb}$. Thus, the activated set ^{198}Au , $^{95}\text{Zr}/^{95}\text{Nb}$, $^{97}\text{Zr}/^{97m}\text{Nb}$ is used to construct three curves for $f(\alpha)$ vs α and every curve consists of a pair of isotopes: ^{198}Au , $^{95}\text{Zr}/^{95}\text{Nb}$; ^{198}Au , $^{97}\text{Zr}/^{97m}\text{Nb}$; and $^{97}\text{Zr}/^{97m}\text{Nb}$, $^{95}\text{Zr}/^{95}\text{Nb}$. The plots of $f(\alpha)$ vs α intersect in a unique point which gives simultaneously α and f .

The specific activity per gram A_{sp} from Eq. (1) is given by:

$$[N_p/(t_m \text{WSDC})]_s = [N_p/(t_m \text{WSDC})]_{\text{au}} \times (k_{0,\text{au}})[(f + Q_{0,s}(\alpha))/(f + Q_{0,\text{au}}(\alpha))], \quad (3)$$

where s and au refers to element and comparator Au. The left hand side of Eq. (3) is the experimental specific activity (A_{sp}), while the right hand side is the theoretical specific activity. In Eq. (3), the nuclear data are lumped in the $k_{0,\text{au}}$ and Q_0 constants [27, 28]. Eq. (3) is for a simple decay code I, however for other complicated decay codes, the terms SDC and $Q_{0,s}$ are modified [27]. It can be converted to the classical well known form after replacing $k_{0,\text{au}}$ by $(\gamma \theta \sigma_0/M)_s/(\gamma \theta \sigma_0/M)_{\text{Au}}$, where M , γ , θ and N_a are the atomic weight, gamma ray intensity, isotopic abundance and Avogadro's number respectively. As a result, Eq. (3) reads

$$(N_p/t_m \text{WSDC})_s = \gamma N_a \theta (\phi_{\text{th}} \sigma_0 + \phi_{\text{th}} I_0(\alpha)/M), \quad (4)$$

and the specific activity for epithermal neutrons ($A_{\text{sp}})_{\text{ep}}$ is given by:

$$(A_{\text{sp}})_{\text{ep}} = \gamma \theta N_a \phi_{\text{ep}} I(\alpha)/M. \quad (5)$$

Experimental procedures

WO_3 (BDH, England), MoO_3 (Ohnson Mathey, England), SnO_2 (Prolabo, France) and TeO_2 (BDH, England) target samples; and Sn, Au, Zr, Ni, Mo and W standards samples were wrapped in clean aluminum foils. The weights of target samples are 21.5, 32, 36.2, and 50.4 mg respectively. The weights of the standard samples are 5.1, 4.3, 4.7, 5.3, 8.6 and 5.7 mg respectively. The targets purity is 99.99 %. The Au (IRMM-530R) is a wire of 0.5 mm and diluted in Al (0.1 % Au), while Zr, Ni, Mo, W and Ni are foils of the purities 99.9 - 99.99 %.

The targets, the standards samples and the IAEA Soil-7 reference sample (30 mg) were irradiated in one of the inner irradiation sites of the second Egyptian research reactor (ETRR-2) for 3 h. After proper cooling times, the aluminum foils surrounding the activated samples were removed and the samples were weighted again. The samples were transferred into clean polyethylene vials for gamma ray measurements.

The gamma ray spectra were collected using a p-type coaxial EG&G Ortec HPGe detector, with 29.4 % relative efficiency and 1.66 keV FWHM at 1332.5 keV of ^{60}Co . A Canberra 10 cm thickness ultra low background lead shield with low carbon steel casing is used in shielding the detector. A guinea card of 16384 channels ADC is mounted on PC for data acquisition and analysis. The absolute efficiency curves of the HPGe detector were previously determined [29]. The samples are

measured after proper cooling times so that, dead times did not exceed 5 %. The measurements were performed at a distance far from the detector head (10 - 15 cm) to minimize true coincidence effects. The measuring times varied from 0.2 to 4 hours. All the calculations (α and f ; and elemental concentrations of the standards and samples) were performed with Excel spreadsheets.

Results and discussion

The epithermal flux index α and the flux ratio f , needed in applying k_0 -NAA method, were determined simultaneously using Eq. (2). The results are shown in Fig. 2. From this figure, α and f were found; 0.06 ± 0005 and 17.3 ± 1 respectively. The average fast neutron flux, ϕ_f over ^{235}U fission neutron spectrum was determined using the reactions: $^{92}\text{Mo} (n, p) ^{92\text{m}}\text{Nb}$, $^{95}\text{Mo} (n, p) ^{95}\text{Nb}$, $^{58}\text{Ni} (n, p) ^{58}\text{Co}$, $^{60}\text{Ni} (n, p) ^{60}\text{Co}$ and $^{90}\text{Zr} (n, 2n) ^{89}\text{Zr}$. The results are shown in Table 1. These reactions are characterized with different threshold energies. It is clearly seen from the determined values that, the fission neutron spectrum is unperturbed.

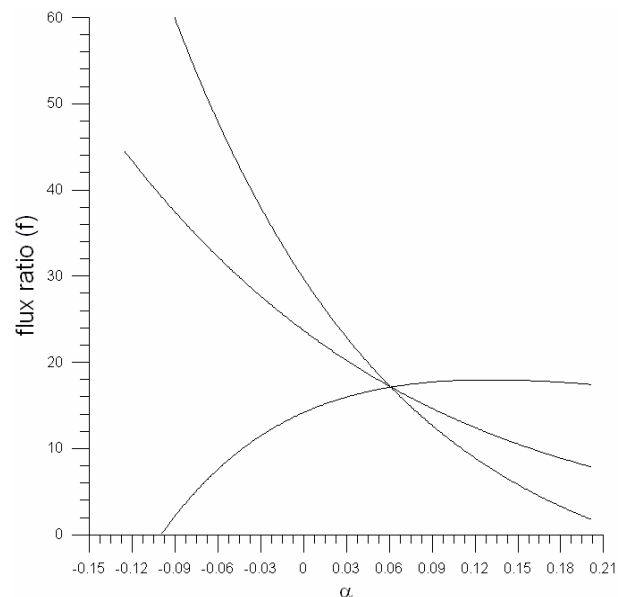


Fig. 2. The flux ratio (f) as a function of α .

The IAEA Soil-7 reference material has been used to check the k_0 -NAA results. The calculated concentrations with their standard deviations, and the comparisons of the calculated and recommended elemental concentrations (% deviation of the calculated from the recommended concentrations, R.E. %) for 16 elements, are shown in Table 2. The calculated concentrations are the mean values arrived from at least three or four measurements. The deviation of the measured concentrations from the reported values is mainly within 10 % except for Cr.

Table 1. Experimental results of determination of fast neutron flux with nuclear data used. Nuclear data were taken from Ref. [30 - 33]

Reaction	Gamma ray energy, keV	Effective threshold energy, MeV	Cross section, mb	Fast flux $\times 10^{13} \cdot n \cdot \text{cm}^{-2} \cdot \text{s}^{-1}$
$^{95}\text{Mo} (n, p) ^{95}\text{Nb}$	765.900	6.6	0.1348 ± 0.0035	2.47 ± 0.21
$^{92}\text{Mo} (n, p) ^{92m}\text{Nb}$	934.440	6	7.3 ± 0.4	2.13 ± 0.17
$^{60}\text{Ni} (n, p) ^{60}\text{Co}$	1173.23 1332.54	6.8	2.31 ± 0.072	2.51 ± 0.23
$^{58}\text{Ni} (n, p) ^{58}\text{Co}$	834	2.6	111 ± 3	2.26 ± 0.15
$^{90}\text{Zr} (n, 2n) ^{89}\text{Zr}$	909.150	12.07	0.104 ± 0.002	2.51 ± 0.25

Table 2. Analytical results of the IAEA-Soil 7

Element	This work \pm S.D	Recommended	Reported 95 % confidence interval	R.E., %
Tb	0.59 ± 0.1	0.60	0.5 - 0.9	5.0
Ta	0.68 ± 0.05	0.80	0.6 - 1.0	0.0
Th	8.28 ± 0.9	8.20	6.5 - 8.7	0.12
Hf	5.20 ± 0.4	5.10	4.8 - 5.5	1.4
Fe (%)	2.65 ± 0.2	2.57*	2.52 - 2.63	3.1
Cr	75.60 ± 3.6	60.00	49 - 74	26
Ce	58.00 ± 0.09	61.00	50 - 63	-4.92
Ba	175.00 ± 3.0	159.00*	131 - 196	10
Cs	5.37 ± 0.17	5.40	4.9 - 6.4	-0.55
Sb	1.52 ± 0.07	1.70	1.4 - 1.8	-10
Rb	51.55 ± 4.7	51.00	47 - 56	-1.1
Co	8.30 ± 0.3	8.90	8.4 - 10.1	-7.2
Sc	8.70 ± 0.3	8.30	6.9 - 9.0	4.9
Yb	2.60 ± 0.03	2.40	1.9 - 2.6	8.3
Nd	27.60 ± 0.06	30	22 - 34	-8
La	26.30	28	27 - 29	-6.07

* Information values.

Table 3. The elemental concentrations (ppm) of radioimpurities in the WO_3 , MoO_3 , TeO_2 and SnO_2 targets determined by k_0 -NAA

Activated product	Half live time	Concentration, ppm			
		WO_3	MoO_3	TeO_2	SnO_2
^{124}Sb	60.1 d	2.16 ± 0.07	0.206 ± 0.01	111 ± 5	238 ± 13
^{60}Co	5.2 y	0.25 ± 0.04	0.081 ± 0.004	0.165 ± 0.004	0.174 ± 0.02
^{182}Ta	114.4 d	11.1 ± 0.4	nd	nd	nd
^{134}Cs	2.065 y	7.6 ± 0.6	nd	nd	nd
^{86}Rb	18.63 d	14	nd	nd	nd
^{95}Zr	64.02 d	nd	168 ± 11	nd	nd
^{233}Pa	26.97 d	nd	0.17	nd	nd
^{65}Zn	244.3	nd	2.087	nd	nd
^{56}Fe	4.5 d	nd	nd	52.7	nd
^{110m}Ag	249.8 d	nd	nd	2.65 ± 0.11	nd
^{75}Se	119.8d	nd	nd	162 ± 5	nd
^{51}Cr	27.7 d	nd	nd	nd	52.2 ± 3
^{114m}In	49.51 d	nd	nd	nd	463 ± 10

Analysis of the gamma ray spectra of the WO_3 , MoO_3 , SnO_3 and TeO_2 irradiated targets showed the following radioimpurities: ^{124}Sb , ^{134}Cs , ^{60}Co , ^{87}Rb , ^{182}Ta , ^{233}Pa , ^{65}Zn , ^{56}Fe , ^{110m}Ag , ^{51}Cr , ^{95}Zr , ^{75}Se and ^{114m}In . The k_0 -NAA was used to determine the concentrations of these radioimpurities. The results

are shown in Table 3. According to the determined impurity concentrations especially ^{114m}In , ^{124}Sb , ^{75}Se and ^{56}Fe (high concentrations), and their half life times, the targets should be chemically purified before neutron irradiations.

In the recorded gamma ray spectra of the irradiated

MoO₃ target (spectra of high count rates), a peak at the gamma rays energy of 320 keV is observed. This peak is due to pile-up (random coincidence or random summing) [34] of 140 - 181 keV gamma rays – it is not of ⁵¹Cr. The 281 keV peak is another example of the pile-up of the 140 - 140 keV gamma rays. These peaks disappear from the spectra with increasing the cooling times since pile-up is proportional with the square of the count rate and does not depend on the geometry of the experiment [34].

Neutron threshold reactions on the stable isotopes of the targets are sources of some impurities and may interfere with neutron capture reactions. With the knowledge of the cross sections over ²³⁵U fission neutron spectrum and the nuclear data of neutron threshold reactions, their contributions to neutron capture reactions were calculated. The contributions of the following reactions: ¹⁸²W(n, p)¹⁸²Ta, ⁹⁸Mo(n, α)⁹⁵Zr, ¹²⁴Te(n, p)¹²⁴Sb, ¹²²Te(n, 2n)¹²¹Te and ¹¹⁴Sn(n, p)^{114m}In reactions are found negligible.

The ratio of the calculated count rate of the ¹⁸⁶W(n, 2n)¹⁸⁵W reaction at the gamma ray line 125 keV of ¹⁸⁵W to the observed one in the recorded gamma ray spectra of the WO₃ target (sum of ¹⁸⁴W(n, γ)¹⁸⁵W and ¹⁸⁶W(n, 2n)¹⁸⁵W reactions) is 0.4. However; the above ratio for ¹⁸²W(n, 2n)¹⁸¹W to the

observed one (produced by ¹⁸⁰W(n, γ)¹⁸¹W and ¹⁸²W(n, 2n)¹⁸¹W reactions) is 0.23. Namely, the ¹⁸⁶W(n, 2n)¹⁸⁵W and ¹⁸²W(n, 2n)¹⁸¹W reactions increase the count rates of the ¹⁸⁴W(n, γ)¹⁸⁵W and ¹⁸⁰W(n, γ)¹⁸¹W reactions by 66 and 30 % respectively. It was not practically possible to determine the Zr concentration in the MoO₃ target via its isotope ⁹⁵Zr at the gamma ray line at 756 keV, because it is obscured by a high Compton background of the ^{92m}Nb nuclide (produced from ⁹²Mo(n, p)^{92m}Nb reaction). Instead, the reaction ⁹⁵Mo(n, p)⁹⁵Nb was used to calculate the count rate of ⁹⁵Nb, which was subtracted from the observed total count rate in the gamma ray spectra and the concentration of ⁹⁵Nb (the decay product of ⁹⁵Zr) was determined. The nuclides ¹²¹Te, ^{121m}Te, ¹²³Te, ¹²⁹Te, ^{129m}Te, and ¹²⁷Te are observed in the TeO₂ irradiated target. Their sources are neutron capture and neutron threshold reactions on the target isotopes of Te. Table 4 shows the cross sections used in the calculations. The values of these cross sections are uncertain and scatter in literature. The cross section values of the ¹²²Te(n, 2n)¹²¹Te and ¹⁸²W(n, 2n)¹⁸¹W reactions are estimated – there are no experimental measurements. Consequently, most of these cross sections should be measured again.

Table 4. The neutron threshold reaction cross sections used in this work. The underline values were used in the calculations

Reaction	Cross section, mb
182-Ta(n,p)182-Ta	<u>0.0038 ± 0.006</u>
186-W(n,2n)185-W	<u>10 ± 0.7</u>
181-W(n,2n)182-W	<u>3.9</u>
Mo-98(n, α) Zr-95	0.00947 ± 0.004, 0.00857 ± 0.00056, <u>0.014 ± 0.002</u> , 0.014 ± 0.0013
Te-124(n, p)Sb-124	<u>0.06 ± 0.005</u>
Te-122 (n,2n)Te-121	<u>0.52</u>
Sn-114(n, p) In-114m	<u>2.37 ± 0.2</u>
Sn-120(n, α) Cd-117	<u>0.14 ± 0.01</u>
Sn-120(n, α) Cd-117m	<u>0.33 ± 0.02</u>
Sn-117 (n, p) In-117	<u>0.13 ± 0.006</u>
Sn-117 (n, n) Sn-117m	140 ± 20 [4], (222 ± 16 [35] , 176 ± 14) [36]
Sn-118(n, 2n) Sn-117m	<u>0.8</u> (estimated) , 1.473
Sn-114(n, 2n) Sn-113	<u>10</u>

Table 5. The experimentally determined and calculated specific activities (Ci/g) and nuclear data used. Nuclear data were taken from Ref. [27, 38]

Isotope	A _{sp} Experimental	A _{sp} Calculated	Decay Code	Contribution of φ _e , %	Q ₀ , Q ₀ (α), I ₀ , I ₀ (α), σ ₀
^{99m} Tc	1.21	1.2	IId	63	53.1, 45.1, 6.96, 5.907, 0.131
^{113m} In	0.14	0.13	Vc	62	48.4, 42.12, 26.2, 23.2, 0.561
^{117m} Sn	0.104	0.096	I	21	56.3, 48.7, 0.336, 0.29, 0.00596
¹³¹ I	0.71	0.78	VIIa	-	1.8, 1.5, 0.342, 0.28, 0.19, σ _{0m} /σ _{0g} = 0.074, Q _{0m} = Q _{0g}
¹⁸⁷ W	9.26	9.82	I	22	13.7, 12.6, 530, 485, 38.7

The nuclides ^{117m}Sn , ^{123}Sn and $^{125}\text{Sn}/^{125}\text{Sb}$ (^{125}Sb is the daughter of ^{125}Sn) are observed in spectra of the irradiated SnO_2 target. Source of ^{123}Sn and ^{125}Sn are neutron capture reactions. ^{117m}Sn is the decay product of the reactions: $^{120}\text{Sn}(n, \alpha)^{117}\text{Cd}$, $^{120}\text{Sn}(n, \alpha)^{117m}\text{Cd}$, $^{117}\text{Sn}(n, p)^{117}\text{In}$ and $^{118}\text{Sn}(n, 2n)^{117m}\text{Sn}$. The contributions of these reactions are 1, 0.3, 0.1 and 0.75 % respectively. ^{117m}Sn is mostly produced by $^{116}\text{Sn}(n, \gamma)^{117m}\text{Sn}$ reaction and the inelastic scattering reaction $^{117}\text{Sn}(n, n')^{117m}\text{Sn}$. The cross section of inelastic scattering reaction was determined using the irradiated Sn standard sample after subtracting the contribution of the reaction $^{116}\text{Sn}(n, \gamma)^{117m}\text{Sn}$. The cross section was determined relative to the fast neutron flux value of $2.5 \cdot 10^{13}$ determined by the reaction $^{58}\text{Ni}(n, p)^{58}\text{Co}$ and found 60 ± 3 mb. This value is smaller than the values reported in literature [4, 35, 36], which are also different from each others. The scatter in the cross section values of this reaction is due to the low neutron threshold energy for this reaction (318 keV). Namely, this cross section depends on the fission neutron spectrum especially in the low energy region. At this region, the spectrum may be disturbed because of neutrons thermalization [37]. In addition, the contribution of the reaction ($^{117}\text{Sn}(n, n')^{117m}\text{Sn}$) to the total activity of both $^{117}\text{Sn}(n, n')^{117m}\text{Sn}$ and $^{116}\text{Sn}(n, \gamma)^{117m}\text{Sn}$ reactions, decreases as the neutron thermalization increases [37].

The specific activity per gram A_{sp} , of the finally produced isotopes were determined experimentally and calculated theoretically using Eq. (3). For the calculation purposes, the determined neutron flux index α was used to correct the Q_0 -values ($Q_0(\alpha) = I_0(\alpha)/\sigma_0$). This factor is so important since the value of $I_0(\alpha)$ may become more or less than the value of I_0 (Table 5). Consequently, this factor should be taken into account when performing such kind of calculations. Fig. 3 shows the variation of Q_0 as a function of the parameter α for $^{116}\text{Sn}(n, \gamma)^{117m}\text{Sn}$ reaction. As α becomes more negative, the value of $Q_0(\alpha)$ increase, namely $I(\alpha)$ increases. This behavior is not only for the $^{116}\text{Sn}(n, \gamma)^{117m}\text{Sn}$ reaction, but also for all other nuclear reactions. As a result, the specific activity due to epithermal neutrons can be increased when irradiation sites, characterized with highly negative values of α are chosen for neutron irradiation.

The contribution of epithermal neutrons to the specific activities was calculated. It is found that their contribution is more than the contribution of thermal neutrons, especially for nuclear reactions characterized with high Q_0 -values. The higher the Q_0 -value, the higher the contribution of the epithermal neutrons to the specific activity, since the

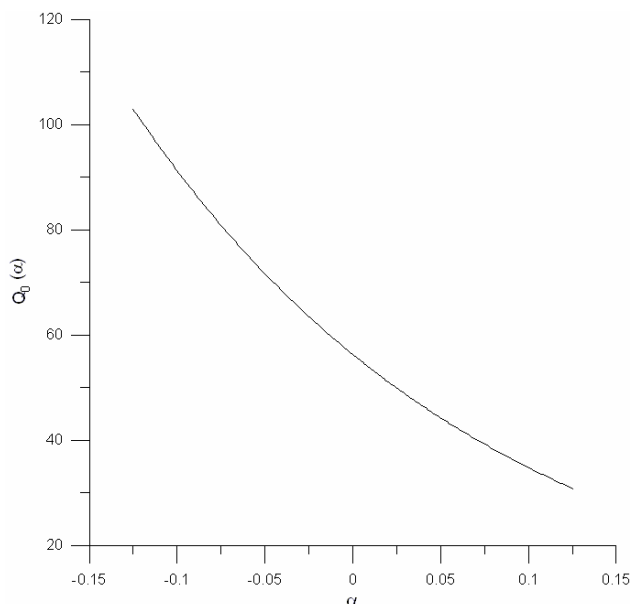


Fig. 3. Variation of $Q_0(\alpha)$ for the $^{116}\text{Sn}(n, \gamma)^{117m}\text{Sn}$ reaction versus α .

smallness of the epithermal flux is compensated by the high Q_0 -value.

The specific activities of the ^{117m}Sn for the irradiated SnO_3 sample due to $^{117}\text{Sn}(n, n')^{117m}\text{Sn}$ and $^{116}\text{Sn}(n, \gamma)^{117m}\text{Sn}$ reactions were determined experimentally and found to be: 0.104 Ci/g. The inelastic reaction contributes by ~ 68 % to the total specific activity. The contribution of epithermal neutrons is ~ 21 %. As a result, epithermal and fast neutrons contribute by ~ 89 % to the total specific activity. This predicts that ^{117m}Sn can be produced with high specific activities in irradiation positions characterized with high fast and epithermal neutron fluxes. Sometimes, in literature the so called effective cross sections are used in calculating the activities [21, 35]. In these calculations, the resonance integrals are not corrected for α – namely $\alpha = 0$. This leads to overestimating the specific activity contributions of epithermal neutrons. In our work setting $\alpha = 0$, increases the specific activities of ^{99m}Tc , ^{113m}In , ^{117m}Sn , ^{131}I and ^{187}W by 17, 13, 16, 22 and 9.3 % respectively.

Novković and Kandić [39] and Alfassi and Groppi [40] calculated the specific activity for ^{199}Au resulting from double neutron capture in ^{197}Au . These calculations were performed for thermal neutrons only. We extend these calculations, to calculate the specific activity of ^{188}W as a result of double thermal and epithermal neutrons captures on ^{186}W . The specific activities of ^{188}W due to thermal neutrons per gram of W, $(A_{\text{sp}})_{\text{th}}$, is given by:

$$(A_{\text{sp}})_{\text{th}} = (\gamma\theta N_a/M)\sigma_1\sigma_2\phi_{\text{th}}[\lambda_2(1 - \exp(-\beta_1 t)) - \beta_1(1 - \exp(-\lambda_2 t))]/[(\lambda_2 - \beta_1)\beta_1], \quad (6)$$

and for epithermal neutrons, it is given by:

$$(A_{sp})_{ep} = (\gamma\theta N_a/M)I_1(\alpha)I_2\phi_{ep}[\lambda_2(1 - \exp(-\beta_2 t_{irr})) - \beta_2(1 - \exp(-\lambda_2 t_{irr}))]/[(\lambda_2 - \beta_2)\beta_2], \quad (7)$$

where $\beta_1 = \lambda_2 + \phi_{th}\sigma_2$, $\beta_2 = \lambda_2 + \phi_{ep}I_2(\alpha)$, λ_1 and λ_2 , σ_1 and σ_2 , $I_1(\alpha)$ and I_2 are the decay constants, thermal neutron cross sections and the resonance integrals of ^{187}W and ^{188}W respectively. The sum of Eqs. (6) and (7) gives the total specific activity of ^{188}W . It was calculated and found to be 1.2×10^{-7} Ci/g ($\sigma_2 = 64$ b and $I_2 = 2760$ b were taken from Ref. [5]; σ_1 and $I_1(\alpha)$ are taken from Table 5. The specific activity of ^{188}W was determined experimentally via ^{188}Re . It is defined as $(A_{sp}) = N_{pRe-188}/(t_m w D C_p)_{s}$, where $N_{pRe-188}$ is the net number of count in the full energy peak (the gamma ray line 633 keV was used) and D is the decay time correction factor given by $\exp(-\lambda_2 t_d)$. A_{sp} was found to be 1.08×10^{-7} Ci/g and in agreement with the calculated result within 10 %. On the other hand, Eqs. (6) and (7) and the experimentally determined specific activity can be used to determine the W content in samples (via ^{188}Re or ^{188}W or both nuclides) with the knowledge of the neutron spectrum parameters and cross sections.

Conclusions

The neutron spectrum parameters characterizing the irradiation position were experimentally determined. The fast neutron flux over ^{235}U was determined using a set of flux monitors. The fast neutron flux in the irradiation position is unperturbed. The accuracy of the k_0 -NAA method was checked by analyzing the IAEA soil-7 reference sample. The radioimpurity concentrations in WO_3 , MoO_3 , SnO_2 and TeO_2 targets were determined using the k_0 -NAA as well as FNAA. Sources of these impurities were identified. Some values of the cross sections are uncertain in literature. It was suggested to purify the targets before neutron irradiation for purpose of radioisotopes production. The specific activities were determined experimentally and theoretically. The contribution of the epithermal neutrons to the total specific activity is higher than the thermal for most isotopes having high Q_0 -values. The higher the negative value of the parameter α for the neutron irradiation site, the higher the specific activity of the produced isotope by epithermal neutrons. The radioisotope ^{117m}Sn can be produced by fast and epithermal neutrons since they constitute 89 of its total specific activity. The theoretically and the experimentally determined specific activities of ^{188}W are found in good agreement.

REFERENCES

1. Moustapha E.M., Ehrhardta J.G., Smith J.C. et al. Preparation of cyclotron-produced ^{186}Re and comparison with reactor-produced ^{186}Re and generator-produced ^{188}Re for the labeling of bombesin // Nuclear Medicine and Biology. - 2006. - Vol. 33. - P. 81 - 89.
2. Knaap F.F., Beets A.L., Mirzadeh S. et al. Production of medical radioisotopes in the ORNL high flux isotope reactor (HFIR) for cancer treatment and arterial restenosis therapy after PICA // Czech. J. Phys. - 1999. - Vol. 49. - Suppl. S1. - P. 799 - 809.
3. Näsam P., Vayrynen T. Impurities in Tc-99m-generators // Eur. J. Nucl. Med. - 1983. - Vol. 8. - P. 26 - 29.
4. Toporov Y.G., Andreyev O.I., Akhetov F.Z. et al. Reactor production of high specific activity Tin-117m at RIAR. // 5th Conf. on Isotopes (Brussels, Belgium, April 25 - 29, 2005).
5. Kuznetsov R.A., Daming C., Pakhomov A.N. et al. $^{188}\text{W}/^{188}\text{Re}$ generators of 1 Ci activity: Results of 7 Month Performance Study. - Ibid.
6. Mostafa M. Purification of neutron-irradiated tellurium targets from cross-radiocontaminants by precipitation with 1,10-phenanthroline // Separation and Purification Technology. - 2009. - Vol. 62. - P. 449 - 457.
7. Prasad D S., Munirathnamt N R., Rao J.V., Prakash T.L. Purification of tellurium up to 5N by vacuum distillation // Materials Lett. - 2005. - Vol. 59. - P. 2035 - 2038.
8. Menhaut W., Adams F., Hoste J. Determination of trace impurities in tin by neutron activation analysis // J. Radioanalytical Chem. - 1970. - Vol. 6. - P. 83 - 95.
9. Menhaut W., Adams F., Hoste J. Determination of trace impurities in tin by neutron activation analysis // Ibid. - 1971. - Vol. 9. - P. 27 - 38.
10. Menhaut W., Adams F., Hoste J. Determination of trace impurities in tin by neutron activation analysis // Ibid. - 1973. - Vol. 14. - P. 295 - 316.
11. Lin C.P., Hsieh B.T., Ting G., Yeh S.J. Determination of impurities in the eluate of rhenium generator using hydrated magnesium oxide as the preconcentration agent // J. Radioanalytical and Nucl. Chem. - 1998. - Vol. 236. - P. 165 - 168.
12. Cosgrove J.F., Morrison G.H. Activation Analysis of Trace Impurities in Tungsten Using Scintillation Spectrometry // Analytical Chem. - 1957. - Vol. 29. - P. 1017 - 1019.
13. Knaap F.F. A generator-Derived Radioisotope for Cancer Therapy // Cancer Biotherapy & radiopharmaceuticals. - 1998. - Vol. 13. - P. 337 - 349.
14. Jun Sig L., Jong-Soup L., UI-Jae P. et al. Development of a high performance $^{188}\text{W}/^{188}\text{Re}$ generator by using a synthetic alumina // Appl. Radiat. Isot. - 2009.

- Vol. 67. - P. 1162 - 1166.
15. *Ryabchikov A.I., Skuridin V.S., Nesterov E.V. et al.* Obtaining molybdenum-99 in the IRT-T research reactor using resonance neutrons // Nucl. Instrum. Methods Phys. Res. B. - 2004. - Vol. 213. - P. 364 - 368.
 16. *Zolle I.* Technetium-99m Radiopharmaceuticals: Preparation and Quality Control in Nuclear Medicine. - Berlin: Springer, 2007.
 17. *Teranishi K., Yamaashi Y., Maruyama Y.* ^{113}Sn - $^{113\text{m}}\text{In}$ generator with a glass beads column // J. Radioanalytical and Nucl. Chem. - 2002. - Vol. 254. - P. 369 - 371.
 18. *Brookeman V.A., Sun P.C.J., Bruno F.P. et al.* Internal distribution and absorbed dose calculations for radioactive indium liver and lung scanning agents // Am. J. Roentgenol. - 1970. - Vol. 109. - P. 735 - 741.
 19. *O'Mara R.E., Subramanian G., McAfee J.G., Burger C.L.* Comparison of $^{113\text{m}}\text{In}$ and other short-lived agents for cerebral scanning // J. Nucl. Med. - 1969. - Vol. 10. - P. 18 - 27.
 20. *Constant-Machadoa H., Leclerc Jean-Pierre, Avilan E. et al.* Flow modeling of a battery of industrial crude oil/gas separators using $^{113\text{m}}\text{In}$ tracer experiments // Chem. Eng. Process. - 2005. - Vol. 44. - P. 760 - 765.
 21. *Ponsard B., Srivastava S.C., Mausner L.F. et al.* Production of Sn-117m in the BR2 high-flux reactor // Appl. Radiat. Isot. - 2009. - Vol. 67. - P. 1158 - 1161.
 22. *Knaap F.F., Mirzadeh S., Beets A.L. et al.* Reactor produced radioisotopes from ORNL for Bone Pain Palliation // Ibid. - 1998. - Vol. 49. - P. 309 - 315.
 23. *Manual for reactor produced radioisotopes*, IAEA-TECDOC-1340. - Vienna: IAEA, 2003.
 24. *Zidan J., Hefer E., Iosilevski G. et al.* // Int. J. of Radiat. Oncology Biology Physics. - 2004. - Vol. 59. - P. 1330 - 1336.
 25. *Van Nostrand D., Wartofsky L.* Radioiodine in the Treatment of Thyroid Cancer // Endocrinology & Metabolism Clinics of North America. - 2004. - Vol. 36. - P. 807 - 822.
 26. *Griggs W.S., Divgi C.* Radioiodine Imaging and Treatment in Thyroid Disorders // Neuroimaging Clinics of North America. - 2008. - Vol. 18. - P. 505 - 515.
 27. *De Corte F., Simonits A.* Recommended nuclear data for use in the k_0 standardization of neutron activation analysis // Atomic Data and Nuclear Data Tables. - 2003. - Vol. 85. - P. 47 - 67.
 28. *Simonits A., Moens L., De Corte F. et al.* k_0 -measurements and related nuclear data compilation for (n, γ) reactor neutron activation analysis. Part I. // J. Radioanalytical and Nucl. Chem. - 1980. - Vol. 60. - P. 461 - 516.
 29. *El Abd A., El-Amir M., Mostafa M.* Implementation of the k_0 -NAA in inner irradiation sites of the second Egyptian Research Reactor (ETRR-2) // Arab J. of Nucl. Sci. and Appl. - 2009. - Vol. 42. - P. 136 - 148.
 30. *Tuli K.J.* Nuclear Wallet Cards. - Brookhaven National Laboratory, National Nuclear Data Center, 2005.
 31. *Chu S.Y., Nordberg H., Firestone R.B., Ekstrom L.P.* Isotope Explorer 2.23, 1999. Data retrieved online up to December 2008.
 32. *Dorval L.E., Arribère M.A., Ribeiro Guevara S. et al.* // J. Radioanalytical and Nucl. Chem. - 2006. - Vol. 270. - P. 603 - 608.
 33. *Calamand A.* Cross-sections for fission neutron spectrum induced reactions // Technical report series No 156: Handbook on nuclear activation cross-sections. - Vienna: IAEA, 1974. - P. 237 - 310.
 34. *Gilmore G.R.* Practical Gamma-ray Spectrometry. - England: John Wiley & Sons Ltd., 2008.
 35. *Mirzadeh S., Knaap F.F., Alexander C.W., Mausner L.F.* Evaluation of neutron inelastic scattering for radioisotope production // Appl. Radiat. Isot. - 1997. - Vol. 48. - P. 441 - 446.
 36. *Mausner L.F., Mirzadeh S., Ward T.E.* Nuclear data for production of Sn-117m for biomedical application // Proc. Int. Conf. on Nuclear Data for Basic and Applied Science. - Santa Fe, NM, 1985. - P. 733 - 737.
 37. *De Corte F., Simonits A., De Weispelaere A., Hoste J.* // J. Radioanalytical and Nucl. Chem. - 1987. - Vol. 113. - P. 145 - 161.
 38. *De Corte F., Simonits A.* k_0 measurements and related nuclear data compilation for (n, γ) reactor neutron activation analysis // Ibid. - 1989. - Vol. 133. - P. 43 - 130.
 39. *Novković D., Kandić A.* The determination of the thermal neutron flux density by the measurement of the activity ratio Au-199/Au-198 // Radiation measurements. - 2004. - Vol. 38. - P. 193 - 195.
 40. *Alfassi Z.B., Groppi F.* On the determination of the thermal neutron flux density by the measurement of the activity ratio Au-199/Au-198 // Ibid. - 2005. - Vol. 39. - P. 561 - 563.

ВИЗНАЧЕННЯ КОНЦЕНТРАЦІЇ ДОМІШОК У ВОЛЬФРАМОВИХ, МОЛІБДЕНОВИХ, ЦИНКОВИХ ТА ТЕЛУРОВИХ МІШЕНЯХ МЕТОДОМ НЕЙТРОННОГО АКТИВАЦІЙНОГО АНАЛІЗУ

А. Ель Абд, М. Мостафа

За допомогою методів активаційного аналізу на швидких нейтронах та k_0 -нейтронах досліджено концентрації радіоактивних домішок ^{124}Sb , ^{134}Cs , ^{60}Co , ^{87}Rb , ^{182}Ta , ^{233}Pa , ^{65}Zn , ^{56}Fe , $^{110\text{m}}\text{Ag}$, ^{51}Cr , ^{95}Zr , ^{75}Se та $^{114\text{m}}\text{In}$ у мішенях зразків WO_3 , MoO_3 , SnO_2 та TeO_2 , необхідних для виробництва радіоактивних ізотопів ^{188}Re , $^{99\text{m}}\text{Tc}$, ($^{113\text{m}}\text{In}$ and $^{117\text{m}}\text{Sn}$) та ^{131}I відповідно на другому єгипетському дослідницькому реакторі (ETRR-2). Описано експериментальні дані, методику експерименту та основи теоретичного підходу. Визначено концентрації радіоактивних домішок та встановлено джерела їх походження - з реакцій захоплення нейтронів або з

пороговых реакций. Точность концентраций, що визначались, перевірялась за допомогою еталонного зразка МАГАТЭ Soil-7.

Ключові слова: домішки, концентрація, ізотоп, потік швидких нейтронів, активність, порогові реакції, k_0 -нейтронний активаційний аналіз, мішень, параметри нейтронних спектрів.

ОПРЕДЕЛЕНИЕ КОНЦЕНТРАЦИИ ПРИМЕСЕЙ В ВОЛЬФРАМОВЫХ, МОЛИБДЕНОВЫХ, ЦИНКОВЫХ И ТЕЛЛУРОВЫХ МИШЕНЯХ МЕТОДОМ НЕЙТРОННОГО АКТИВАЦИОННОГО АНАЛИЗА

А. Эль Абд, М. Мостафа

При помощи методов активационного анализа на быстрых нейтронах и k_0 -нейтронах исследованы концентрации радиоактивных примесей ^{124}Sb , ^{134}Cs , ^{60}Co , ^{87}Rb , ^{182}Ta , ^{233}Pa , ^{65}Zn , ^{56}Fe , $^{110\text{m}}\text{Ag}$, ^{51}Cr , ^{95}Zr , ^{75}Se и $^{114\text{m}}\text{In}$ в мишенях образцов WO_3 , MoO_3 , SnO_2 , TeO_2 , необходимых при производстве радиоактивных изотопов ^{188}Re , $^{99\text{m}}\text{Tc}$, ($^{113\text{m}}\text{In}$ and $^{117\text{m}}\text{Sn}$) и ^{131}I соответственно на втором египетском исследовательском реакторе (ETRR-2). Описаны экспериментальные данные, методика эксперимента и основы теоретического подхода. Определены концентрации радиоактивных примесей и установлены источники их происхождения - из реакций захвата нейтронов или из пороговых реакций. Точность определяемых концентраций проверялась при помощи эталонного образца МАГАТЭ Soil-7.

Ключевые слова: примеси, концентрация, изотоп, поток быстрых нейтронов, активность, пороговые реакции, k_0 -нейтронный активационный анализ, мишень, параметры нейтронных спектров.

Received 12.11.09,
revised - 16.12.09.